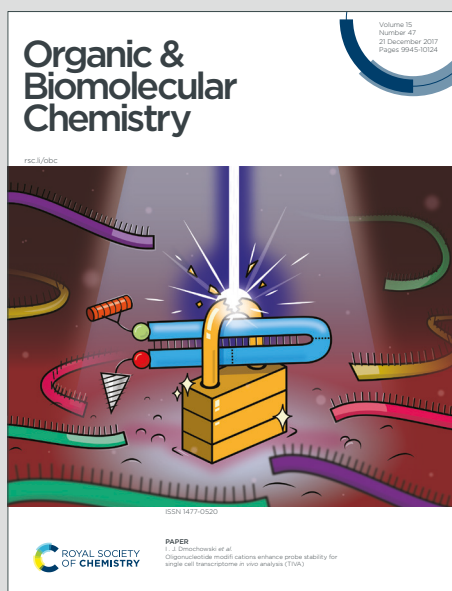


Organic & Biomolecular Chemistry

Accepted Manuscript

This article can be cited before page numbers have been issued, to do this please use: D. Padula, G. Mazzeo, E. Santoro, P. Scafato, S. Belviso and S. Superchi, *Org. Biomol. Chem.*, 2020, DOI: 10.1039/D0OB00052C.



This is an Accepted Manuscript, which has been through the Royal Society of Chemistry peer review process and has been accepted for publication.

Accepted Manuscripts are published online shortly after acceptance, before technical editing, formatting and proof reading. Using this free service, authors can make their results available to the community, in citable form, before we publish the edited article. We will replace this Accepted Manuscript with the edited and formatted Advance Article as soon as it is available.

You can find more information about Accepted Manuscripts in the [Information for Authors](#).

Please note that technical editing may introduce minor changes to the text and/or graphics, which may alter content. The journal's standard [Terms & Conditions](#) and the [Ethical guidelines](#) still apply. In no event shall the Royal Society of Chemistry be held responsible for any errors or omissions in this Accepted Manuscript or any consequences arising from the use of any information it contains.

ARTICLE

Amplification of the Chiroptical Response of UV-transparent Amines and Alcohols by *N*-Phthalimide Derivatization Enabling Absolute Configuration Determination through ECD Computational Analysis[†]

Received 00th January 20xx,
Accepted 00th January 20xx

DOI: 10.1039/x0xx00000x

Daniele Padula,^{a,b,‡} Giuseppe Mazzeo,^{a,c,‡} Ernesto Santoro,^{a,‡} Patrizia Scafato,^a Sandra Belviso,^a and Stefano Superchi^{a,*}

The stereoselective transformation of chiral UV-transparent amines and alcohols to phthalimides has been proved to be a simple and efficient method to enhance the chiroptical response of these substrates allowing their reliable absolute configuration determination by computational analysis of ECD spectra. Such transformation also leads to a significant reduction of the molecular conformational flexibility thus simplifying the conformational analysis required by the computational treatment. The method described herein thus allows the absolute configuration assignment to these challenging substrates to be much easier and reliable.

Introduction

The assignment of the molecular absolute configuration (AC) is a fundamental task to be addressed when dealing with chiral molecules. Among the several approaches nowadays available for the AC assignment, the use of chiroptical spectroscopies, i.e. optical rotation (OR) and optical rotatory dispersion (ORD), electronic circular dichroism (ECD) and vibrational circular dichroism (VCD) has emerged as one of the most versatile and reliable.¹ As a matter of fact, chiroptical measurements are usually quite rapid to perform, can be carried out in solution, thus allowing to treat also non crystalline compounds, and often allow to analyse very small amounts of compound, a frequent situation when dealing with products coming from natural sources.² In particular, ECD and ORD spectroscopies, whose measurements are performed in the UV-visible spectral range, have the advantage to display higher sensitivity, thus allowing microscale measurements, to require more accessible

instrumentation, and to allow easier and faster data acquiring compared to VCD.³ The use of such spectroscopies for AC assignments has been also enormously fuelled by the recent advances in the development of *ab initio* predictions of chiroptical properties^{4,5} which led to quantum-chemical calculation of OR⁶/ORD,⁷ ECD,⁸ and VCD⁹ data. This is demonstrated, for example, by the large number of papers published in these last few years where the AC of natural compounds¹⁰ has been determined thanks to these techniques¹¹ or their concerted use.^{11b,c,f,g,12} However, despite the significant progresses carried out in this field, the treatment of molecules devoid of chromophores and thus nearly UV-transparent still remains a quite challenging task for ORD and ECD spectroscopies. These compounds, in fact, show low ORs and/or weak ECD spectra making unreliable any attempt of their computation.¹³ This is the case of aliphatic molecules having only non-chromophoric functional groups like ethers, alcohols, and amines, often encountered in natural products. Moreover, the difficulties are even greater in case of conformationally flexible molecules, displaying many conformers with different (or even opposite) values of chiroptical properties simultaneously present. In fact, all the computational approaches above, require averaging of the calculated specific chiroptical property over the exact conformer distribution and therefore the knowledge of the conformers structure and distribution. It follows that when treating molecules displaying high conformational mobility, the conformational analysis is very difficult and time-consuming and some uncertainties on the AC determination can arise. Both problems can be overcome resorting on introduction of a suitable chiroptical probe onto the molecule under investigation, i.e. introducing a chromophoric moiety which gives rise to ORD and ECD signals which can be reliably

^a Dipartimento di Scienze, Università della Basilicata, via dell'Ateneo Lucano, 85100; Potenza, Italy.

^b Present address: Dipartimento di Biotecnologie, Chimica e Farmacia, Università di Siena, via A. Moro 2, 53100; Siena, Italy.

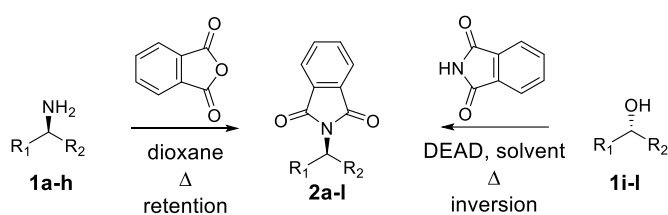
^c Dipartimento di Medicina Molecolare e Traslazionale, Università di Brescia, Viale Europa 11, 25123; Brescia, Italy.

[†]Dedicated to our friend and mentor Carlo Rosini on the 10th anniversary of his death.

[‡]These authors contributed equally to the work.

Electronic Supplementary Information (ESI) available: ORD and ECD spectra; conformers structure. See DOI: 10.1039/x0xx00000x.

correlated either qualitatively or quantitatively with molecular AC, possibly also reducing its conformational mobility.¹⁴ In the last years our group developed several approaches to assign AC of flexible molecules by ECD spectroscopy, introducing the use of biphenyl-based chiroptical probes for UV-transparent chiral diols,¹⁵ carboxylic acids,¹⁶ and amines,¹⁷ the use of biphenyl boronates for mono aryl-substituted diols,¹⁸ and applying the fluorene,¹⁹ triaryl,²⁰ and *p*-bromobenzoate^{11f} chromophores for the enhancement of chiroptical properties of diols and naturally occurring alcohols, respectively. We now disclose herein a novel type of derivatization by the phthalimide chromophore, which allows enhancement of the ORD and ECD chiroptical response of UV-transparent monofunctional amines and alcohols (Scheme).²¹ *N*-phthaloyl derivatization is a common protection method employed for primary amino groups in organic synthesis.²² It was also proposed by Gawroński *et al.* to obtain bis-chromophoric derivatives²³ of diamines²⁴ or amines bearing a second chromophore²⁵ allowing to determine AC by the exciton chirality approach.²⁶ Such moiety displays several peculiar advantages over other possible chromophoric probes. First of all, it is easily introduced by stereospecific reactions on the substrates, i.e. with retention of configuration in amines and inversion in alcohols (*vide infra*) (Scheme). Secondly, it has been fully characterized by the spectroscopic point of view and the nature and polarization of its transitions are well known. It displays five $\pi \rightarrow \pi^*$ transitions in the 200-300 nm range, three of which being polarized along the short axis, at 210 nm, 235 nm ($\epsilon \sim 12000$), and 275 nm ($\epsilon \sim 500$), two polarized along the long axis at 220 nm ($\epsilon \sim 33000$) and 300 nm ($\epsilon \sim 1800$), and a weak $n \rightarrow \pi^*$ low energy transition at 320-340 nm ($\epsilon \sim 100$).^{24,27} Such transitions can give rise to well visible Cotton effects in the UV region. Most importantly, this chromophoric moiety is fully planar and its long axis is directed along the single bond linking it to the substrate. As a consequence, it displays cylindrical symmetry under N-C* bond rotation. It follows that upon derivatization the number of rotationally free bonds on the molecule and thus the number of accessible conformers is decreased with respect to the parent compounds. From this point of view such derivatization appears superior to the common *p*-bromobenzoate derivatization where two new rotationally free bonds are added. As shown below, introduction of such moiety gives rise to a strong enhancement of both ORD values and ECD spectra of amines and alcohols also reducing the number of conformers in respect to the parent compounds. This allows a reliable computation of the chiroptical properties, thus arriving at a safer AC assignment.



Scheme 1. Reaction pathways of transformation of alcohols and amines in phthalimides.

Results and discussion

The ability of the phthaloyl chromophore to enhance the chiroptical response of UV-transparent chiral compounds was tested on known chiral amines, aminoacids, and carbinols chosen as benchmark molecules (Chart 1, compounds **1a-l**).

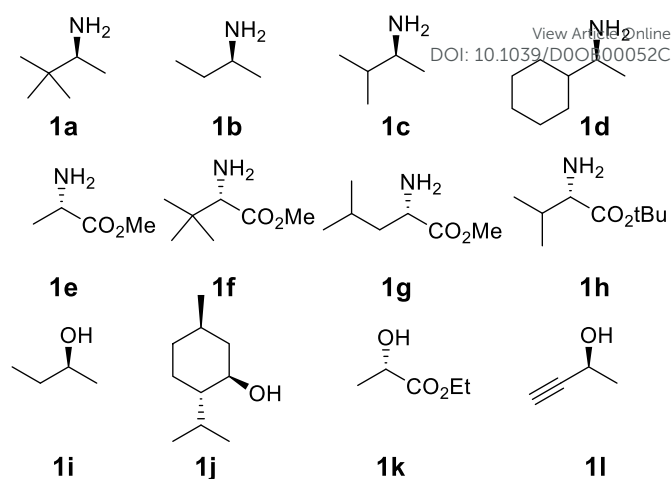


Chart 1. Benchmark molecules with known AC used in this work.

These compounds represent different classes of molecules: **1a-d** are primary aliphatic amines with substituents on the stereocentre of increasing size, **1e-h** are α -aminoesters, chosen to evaluate the impact of a second, weak, chromophore on the optical response, **1i** and **1j** are chiral secondary alcohols, **1k** is an α -hydroxyester and **1l** is a propargylic alcohol, again chosen to evaluate the effect of a second weak chromophore. All these compounds are devoid of chromophores giving rise to UV absorption above 205 nm, therefore they display extremely weak ECD spectra and quite low specific OR (SOR) values at 589 nm (wavelength of sodium D line), i.e. $[\alpha]_D$ values. This situation often leads, as stated above, to uncertain AC assignment by computational analysis of these chiroptical properties. For example, in compound **1a**, which is the most rigid amine in the set (3 populated conformers at room temperature), the computational prediction of OR at TDDFT/B3LYP/6-31G* level of theory, gives a value of $[\alpha]_D = -7$, opposite to the experimental value which is $[\alpha]_D = +25$. Even employing a higher TDDFT/B3LYP/aug-cc-pVDZ level of computations for both the geometry optimization and OR calculation a wrong $[\alpha]_D = -2$ is obtained, demonstrating that even heavy calculations may be not enough for treating of such systems.

These results highlight that the direct AC assignment on such compounds is unsafe and an enhancement of their chiroptical response is needed, as allowed by addition of the chromophoric phthaloyl moiety to **1a-l**.

Amines **1a-h** were then transformed in the corresponding phthalimides **2a-h** (Chart 2) by reaction with phthalic anhydride (Scheme), while carbinols **1i-l** were transformed in phthalimides **2i-l** by Mitsunobu reaction²⁸ with phthalimide (Scheme). In the latter case Mitsunobu reaction gives rise to a stereospecific inversion at the stereogenic centre, leading to chiral phthalimides of opposite AC with respect to the parent alcohols.

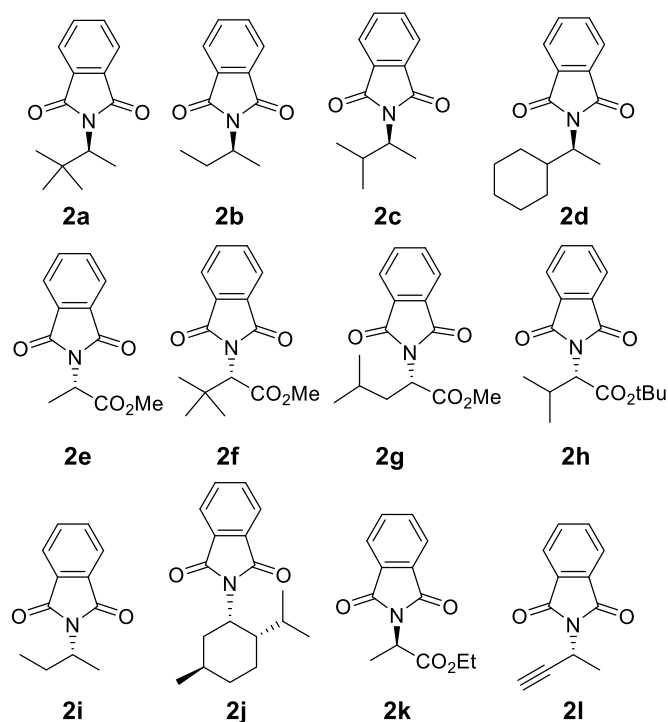


Chart 2. Phthalimides derivatives of benchmark compounds 1a-l.

The $[\alpha]_D$ values for compounds **2a-l** were then measured in chloroform. Experimental $[\alpha]_D$ for compounds **2a-l** are not particularly intense: they have medium-low values between 10-20 units (Table S1 in Electronic Supplementary Information, SI). The only exception is phthalimide **2f**, showing a higher $[\alpha]_D$ value of -58 . The expected enhancement of the $[\alpha]_D$ upon derivatization did not occur, or at least not as expected. Additionally, the SOR values are not so high to guarantee a safe AC assignment by sole SOR calculations. A signal enhancement is instead observed in the ORD curves except for the **1l/2l** couple (Figures S1-S4 in ESI). In some cases, we measured rotatory power values in different solvents, obtaining consistent results (see Table S2 in ESI) demonstrating the low impact of the solvent environment on the chiroptical measurements. The negligible solvent impact on the chiroptical experimental values allowed us to carry out calculations only in gas-phase avoiding more computationally demanding methods for the inclusion of solvent effects, such as implicit PCM²⁹ model or explicit solvent models.³⁰ On the contrary, the introduction of the chromophoric unit strongly enhanced the chiroptical response in the UV range, giving rise to relatively intense ECD spectra for all the phthalimides and thus allowing to employ ECD for a safe AC assignment (see for example Figures S5-S6 in ESI). Also, ECD spectra appeared independent from the solvent environment, allowing to overlook solvation in the computations. We obtained ORD curves for compounds **2a-l** (see Figures S20 and S21 in ESI) measuring the rotatory power at different wavelengths (namely, 589 nm, 546 nm, 435 nm, 405 nm). Rotatory power values at lower wavelengths are more reasonable for a safe AC assignment, varying in the range between 20-70 units for all the phthalimides. The experimental ECD profiles are consistent in each series of compounds

showing structural analogies (see Figures S22 and S23 in ESI). All phthalimides **2a-d** show a weak broad positive Cotton effect at 290 nm ($\Delta\epsilon \sim +0.5$). In **2b** a series of opposite-in-sign bands is present in the 240-190 nm region of the ECD spectrum (Figure 3): a low intensity ($\Delta\epsilon = -1.0$) negative signal at 240 nm, a positive signal at 220 nm ($\Delta\epsilon = +2.0$) and a negative band at 200 nm ($\Delta\epsilon = -0.5$). The same spectral pattern is observed in **2c**, **2d**, and, as a mirror image, in phthalimides **2i**, **2j**, and **2l** (Figure S23 in ESI), having opposite AC at the stereocentre bearing the phthaloyl chromophore. Considered that the only chromophore present in these molecules is the phthalimide moiety, it is reasonable to ally such bands to the $\pi \rightarrow \pi^*$ transitions of such chromophore, as discussed in the Introduction. In case of phthalimide **2a**, we noticed a vibronic progression with sign inversion patterns in the low energy region of the spectrum,³¹ but the detailed analysis of this interesting spectral feature is beyond the aims of the present work. Phthalimides **2e-h**, derived from aminoesters, showed more intense spectra (Figures S22 and S23 in ESI) characterized by a sequence of two opposite-in-sign Cotton effects at 220 nm ($\Delta\epsilon = -10$) and 210 nm ($\Delta\epsilon = +5$) which can be allied to the $\pi \rightarrow \pi^*$ phthalimide transition at 225 and the $n \rightarrow \pi^*$ transition of the carboxyl moiety at 205 nm. As expected, the same pattern was observed for compound **2k**, derived from a hydroxy acid and practically enantiomeric to **2e**.

Computation of ORD curves and ECD spectra was then carried out to verify if the phthalimide derivatization could allow a reliable spectral reproduction eventually leading to a safe AC assignment. We then first performed a preliminary conformational search on compounds **2a-l** by molecular mechanics (MMFF94s force field). The obtained geometries were then re-optimized at DFT/B3LYP/TZVP level of theory (Figure 1 and Figures S7-S17 in ESI). The optimization results show a good agreement with structures experimentally obtained by Gawroński by X-ray diffraction:²⁴ in fact, in all the compounds the most stable conformation is the one in which the phthalimide moiety is eclipsed with respect to the hydrogen on the stereocentre (Figure 1 and Figures S7-S17 in ESI). The conformational search also shows that the phthalimide derivatization strongly reduces the conformational mobility of the compounds, decreasing the number of populated conformers with respect to the parent amines and alcohols (Table S1 in ESI). For example, the MM conformational search provided 9 conformers for the free amine **1b** and only 3 for the corresponding phthalimide **2b**. After DFT optimization, the first

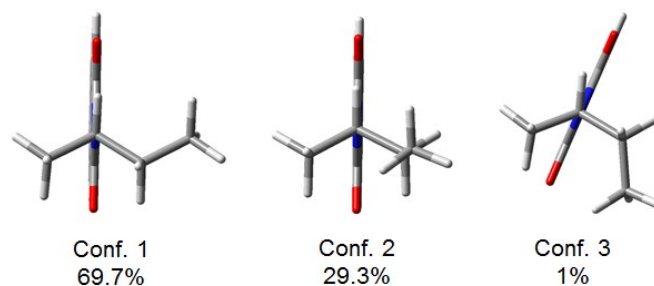


Figure 1. Structures and Boltzmann populations (room temperature) of the conformers (DFT/B3LYP/TZVP) of compound **2b**.

two conformers of **2b** accounted for the 99% of the Boltzmann population at room temperature (Fig. 1), making possible to neglect the third one. As representative examples of the different phthalimides subclasses, the results obtained for compounds **2b** and **2f** are discussed in further detail. The $[\alpha]_D$ value increases upon derivatization from +7 (for **1b**) to +17 (for **2b**). Even if the enhancement in the $[\alpha]_D$ value is not as high as expected, it certainly allows a safe configurational assignment because it is accompanied by a great reduction of the number of populated conformers (Table S1 in ESI). Calculations of SOR at TDDFT/B3LYP/aug-cc-pVDZ give positive values for all conformers of **2b**, making the assignment of AC straightforward and independent from the quality of the conformational analysis performed. The Boltzmann-averaged value is +24, showing a good qualitative and quantitative agreement with the experimental one which is +17.

We observed a similar situation looking at the calculated structures and SOR data for other compounds belonging to the same subclass, apart from the existence of conformers with negative OR values (**2a-d**, see ESI). The experimental ORD curve of **2b** (Figure 2) appears as a positive monotone curve, showing an increasing behaviour upon approaching to the absorption wavelength. The simulated ORD curve obtained by computing the SOR values at the desired wavelengths shows a good agreement with the experimental profile (Figure 2). The introduction of the phthalimide chromophore makes it possible to perform also an independent AC assignment by ECD spectroscopy. We performed calculations of oscillator and rotatory strengths of **2b** at TDDFT/CAM-B3LYP/aug-cc-pVDZ level for each conformer and obtained the Boltzmann averaged UV and ECD spectra. The ECD spectrum shows a very good overlap with the experimental one (Figure 3), satisfactorily reproducing the position (after UV correction) and intensity of the main bands, thus allowing a safe AC assignment. We then turned out to phthalimide **2f**, belonging to the subclass of compounds endowed with a second weak chromophore. MM conformational analysis of this substrate reveals the presence

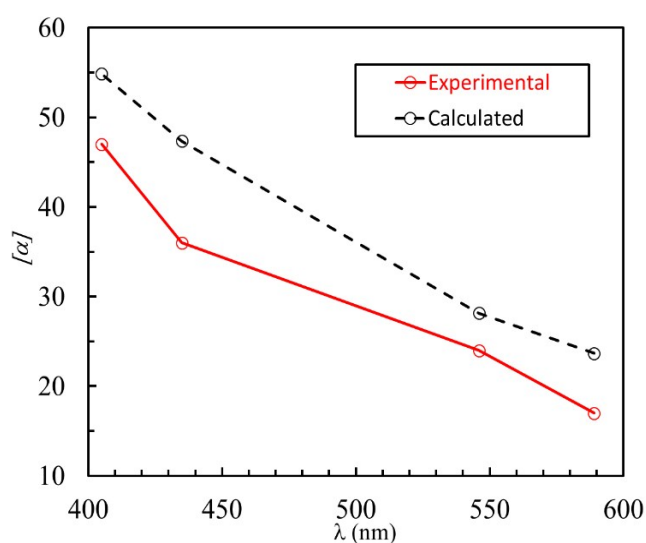


Figure 2. Comparison between experimental and calculated (TDDFT/B3LYP/aug-cc-pVDZ) ORD curves for compound **2b**.

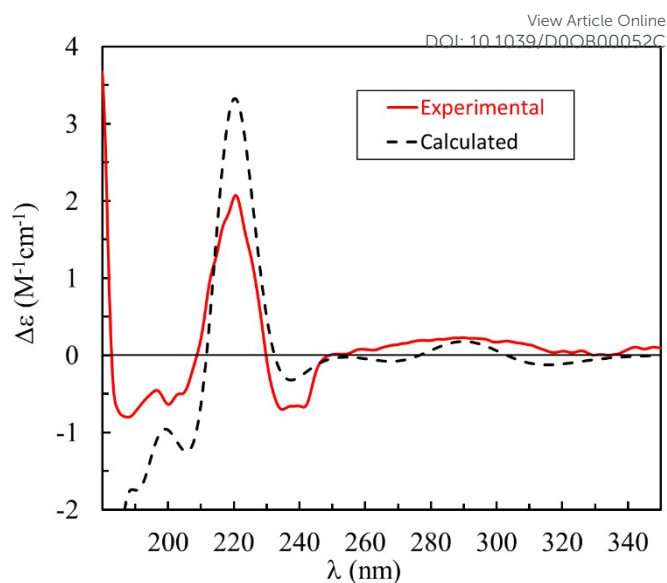


Figure 3. Comparison between experimental and calculated (TDDFT/CAM-B3LYP/aug-cc-pVDZ, $\sigma = 0.20$ eV, UV correction = + 20 nm) ECD spectra for compound **2b**.

of 3 populated conformers, while 7 were displayed by the parent compound **1f** (Table S1 in ESI). After DFT optimization, the conformers of **2f** reveal to be only 2, with the major one accounting for 90.6% of the Boltzmann population. The main structural difference between the two conformers is the orientation of the ester group (Figure 4). In general, compounds belonging to the same subclass of **2f** (i.e. **2e-h**) show a higher number of conformers with respect to other subclasses (**2a-d**) due to the presence of the flexible ester group (Table S1 in ESI), which can assume two conformations (*s-cis* and *s-trans*) with respect to the phthalimide moiety. Going along this subclass, the number of conformers gradually increases (2, 2, 5, and 7 for **2e-h** respectively), and in all cases the major conformer shows an *s-trans* arrangement (Figures S11-S14 in SI). Additionally, the *s-trans* conformation characterizes also the majority of other conformations: more specifically, for **2g**, 4 out of 5 conformers (accounting for 63.8% of the total) show an *s-trans* arrangement. For **2h**, the count is 3 conformers out of 7 (accounting for 72.4% of the total). Upon derivatization, the $[\alpha]_D$ changes from +61 for **1f** to -58 for **2f**, showing a sign inversion, although the AC of the stereocenter remains the same. The two conformers show opposite sign in all the calculated chiroptical properties: therefore, in this case, the configurational assignment is strongly dependent on the quality

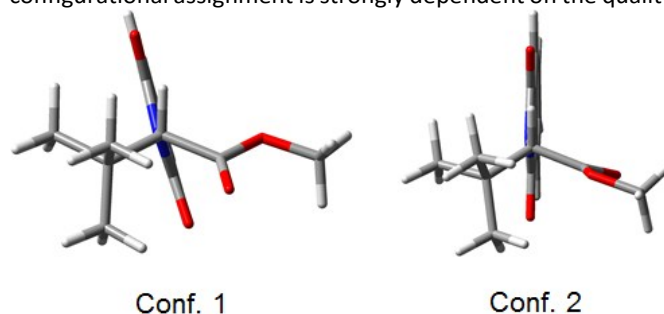


Figure 4. Structures and Boltzmann populations (room temperature) for the two conformers of compound **2f**.

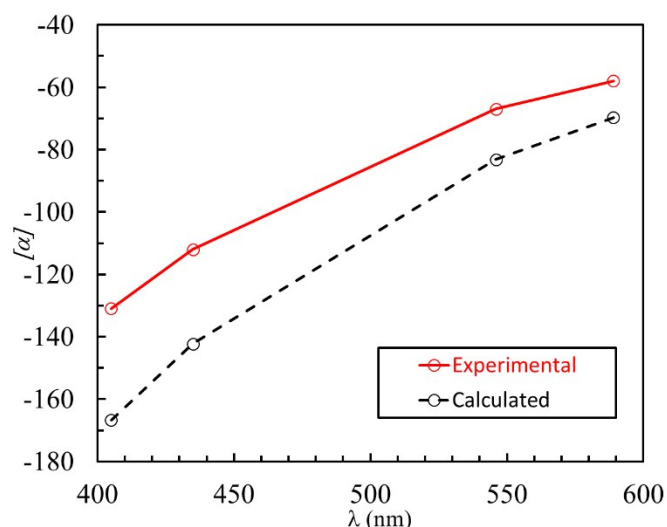


Figure 5. Comparison between experimental and calculated (TDDFT/B3LYP/aug-cc-pVDZ) ORD curves for compound **2f**.

of the conformational analysis. The computed Boltzmann-averaged value for the $[\alpha]_D$ is -70 , in very good agreement with the experimental one (-58). A good agreement is also noticed along the whole ORD curve for this compound (Figure 5). The comparison between the experimental and Boltzmann-averaged computed ECD spectra for **2f** are reported in Figure 6, together with the spectra of the two stable conformers found. Although these two conformers show mirror-like behaviour, the total spectrum shows a very good agreement with the experimental one, providing an independent configurational assignment and once more a confirmation of the good quality of the performed conformational analysis. It is interesting to note that, while conformers showing a similar arrangement (*s-cis* or *s-trans*) of the ester moiety show consistent ECD spectra, the same does not happen for the SOR. For example, in compound **2g**, while the ECD spectra of all *s-trans* conformers are almost perfectly superimposable, only the major *s-trans* conformer shows a positive value of SOR, while the other give

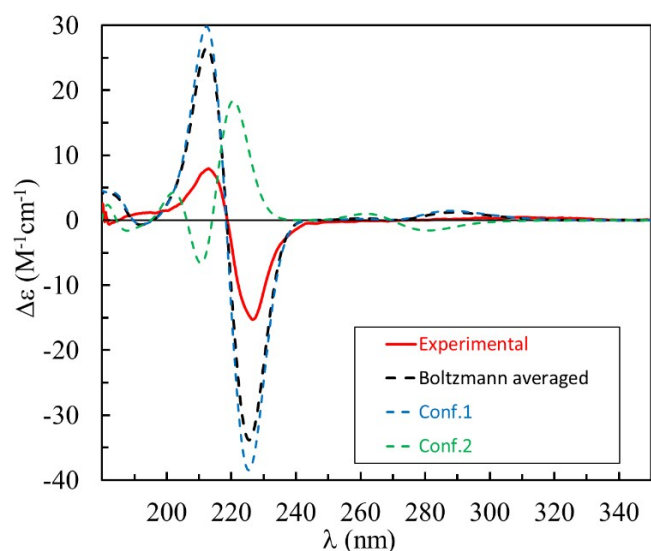


Figure 6. Comparison between experimental and calculated (TDDFT/CAM-B3LYP/aug-cc-pVDZ, $\sigma = 0.20$ eV, UV correction = +10 nm) ECD spectra for compound **2f**.

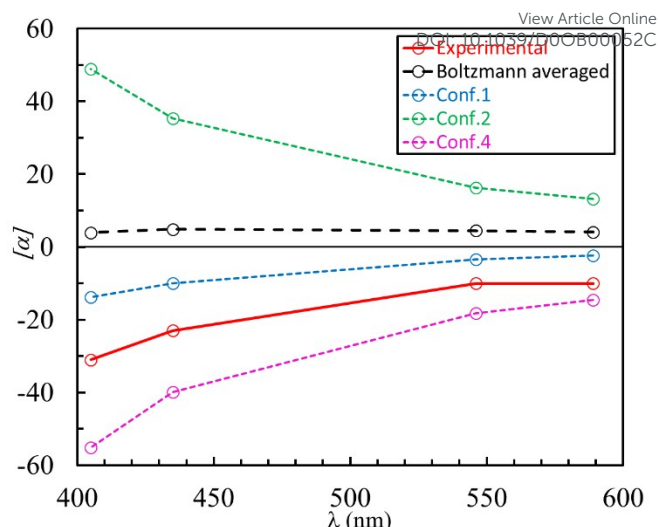


Figure 7. Comparison between experimental and calculated (TDDFT/B3LYP/aug-cc-pVDZ) ORD curves for compound **2h**.

negative SOR. For **2h**, we noticed a similar structure/properties picture for the conformers, with even higher impact on the Boltzmann-averaged chiroptical properties: even high-level calculations fail to predict the correct AC by SOR calculation at 589 nm, and the calculated ORD curve appears opposite in sign in respect to the experimental even at lower wavelengths (Figure 7). On the other side, the Boltzmann-averaged ECD spectrum gives a very good agreement with experiment (Figure 8). For **2k**, the prediction of the ORD, as well as the ECD, show a good agreement with the experiment (see Figures S21 and S23 in ESI). The possibility to have even higher chiroptical properties enhancement by using a stronger and more extended chromophore like the naphthimide was also checked. However, the naphthimide derivatization did not provide significant advantages over phthalimide. In fact, the naphthimide **3b** derived from **1b** displayed a negligible enhancement of the ORD curve and a more complex ECD spectrum than **2b** (Figures S18 and S19 in ESI).

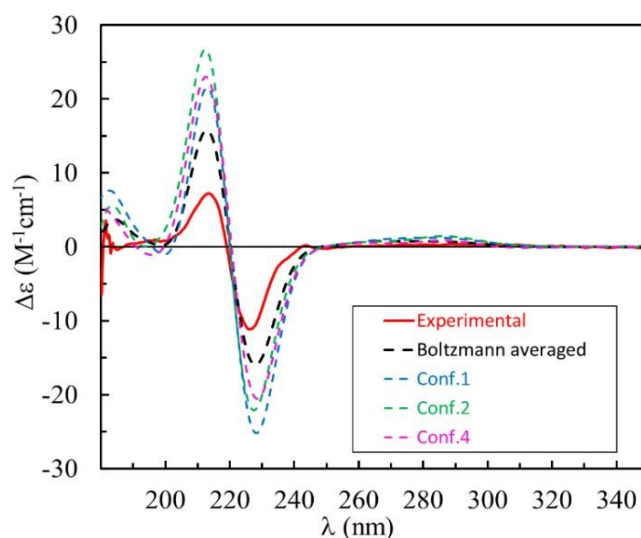


Figure 8. Comparison between experimental and calculated (TDDFT/CAM-B3LYP/aug-cc-pVDZ, $\sigma = 0.20$ eV, UV correction = +10 nm) ECD spectra for

Conclusions

Flexible and transparent systems represent a big challenge for the AC assignment based on the computational analysis of chiroptical properties. In fact, in the presence of high number of conformers and of weak chiroptical properties, even high-level calculations might lead to ambiguous results. The presence of a reactive functional group allows taking advantage of its chemistry for introducing a suitable chromophore, which enhances the chiroptical response in the derivative: higher values of OR are usually measured, and independent studies can be performed by ECD, thanks to the presence of electronic transitions in the UV region. This way, the AC can be assigned at least through two different independent methods.

We demonstrated herein that derivatization of amines and alcohols **1** to form phthalimides **2** leads to (i) in most cases a significant reduction of the conformational flexibility (ii) a slight enhancement of the optical rotatory values and (iii) the appearance of moderate to intense signals in ECD. This makes the computation of such chiroptical properties much easier and reliable as it is the resulting AC assignment.

Additionally, we thoroughly discussed the topic of structure/properties relationships for compounds **2**, showing that ORD in some cases fails to predict the correct AC, while ECD appears to be a superior and more reliable tool which has to be recommended for future applications.

Experimental

Computational Details

The structures to be used as starting geometries in the QM optimizations were generated by means of a conformational analysis with the Spartan '02 software,³² using both the systematic and Montecarlo methods in combination with molecular mechanics (MMFF94s force field) and retaining only the structures within 4 kcal/mol from the minimum.³³ All the resulting geometries were fully optimized at the DFT/B3LYP/TZVP level in the gas phase using the Gaussian 09 package.³⁴ All conformers are real minima; no imaginary vibrational frequencies were found. In all cases, the free energy values at T = 298 K were employed to calculate the population of each conformer, using the Boltzmann statistics. The calculations of the optical rotatory power were carried out at TDDFT/B3LYP/aug-cc-pVDZ basis sets level in gas phase. The theoretical values of specific optical rotation (to be compared with the experimental ones) were obtained as weighted averages on the Boltzmann populations calculated in the gas phase, for each wavelength at which the calculation was performed. Rotatory strength calculations were carried out at the TDDFT/CAM-B3LYP level with both TZVP and aug-cc-pVDZ basis sets in gas phase. To guarantee origin independence and to evaluate the quality of the molecular wave functions employed, calculated ECD spectra were obtained both in the length and velocity form, using the lowest 30 states. In all cases the velocity/length calculated spectra were almost coincident, indicating a good level of calculation. Therefore, in all Figures only the velocity-form predicted spectra are reported. The

simulated ECD spectra were obtained using overlapping Gaussian functions with a width $\sigma = 0.20$ eV with the software SpecDis.³⁵ In the comparison of computed ECD spectra with the experimental a wavelength correction⁹ of +10÷20 nm has been applied.

General procedures

All reactions were performed in flame-dried glassware under nitrogen, unless noted. Chloroform was refluxed over P₂O₅ and distilled under nitrogen atmosphere before its use. THF was heated at reflux over sodium/benzophenone and distilled under nitrogen atmosphere before use. Chromatographic separations were carried out on suitable dimension columns using Merck 60 silica gel (70-230 mesh). Analytical thin-layer chromatography (TLC) was performed on Macherey-Nagel aluminum sheets precoated with silica gel (0.2 mm). NMR spectra were recorded in CDCl₃ on a 300, 400 or 500 MHz NMR spectrometer using TMS as the internal standard and are reported in parts per million (ppm) relative to TMS (0), with coupling constants (*J*) in hertz. Optical rotatory powers were measured with a digital polarimeter Jasco DIP-370, using standard cuvettes (*l* = 1.0 dm). Gas chromatographic analyses and mass spectra (EI) were carried out on GC/MS GC-HP 6890 plus chromatograph equipped with a mass selective detector HP 5973 and a capillary column (30 m × 0.25 mm, 5% phenyl methyl siloxane as stationary phase) using helium as carrier gas. Absorption and ECD spectra were recorded by a J-815 spectropolarimeter, with a concentration of c.a. 10⁻³M in a 0.1mm pathlength cell. Melting points were measured with a Scientific SMP3 apparatus and are uncorrected. Unless otherwise noted, commercially available compounds, **1a-l** were used without further purification.

General procedure for the preparation of Phthalimides **2a-h**

To a solution of phthalic anhydride (296 mg, 2 mmol) in 5 mL of dioxane, 2 mmol of amine **1a-h** were added. The reaction mixture was stirred under reflux until consumption of phthalic anhydride. After evaporation of the solvent under reduced pressure, the crude was purified by column chromatography on silica gel (petroleum ether/Et₂O 1:1).

General procedure for the preparation of Phthalimides **2i-l**

To a solution of PPh₃ (788 mg, 3 mmol) and phthalimide (446 mg, 3 mmol) in 10 ml of THF, 3 mmol of alcohol **1i-l** are added. DEAD (547 μL, 3 mmol) is then slowly added, and the reaction mixture is left at reflux overnight. After evaporation of the solvent under reduced pressure, 3 fractions of 50 mL each of Et₂O are added to the crude, and the white precipitate is removed by filtration. The Et₂O is then removed under reduced pressure and the crude purified by column chromatography on silica gel (petroleum ether/Et₂O 5:1).

(S)-2-(3,3-dimethylbutan-2-yl)isoindoline-1,3-dione (2a) yield 25%; m.p.=64–66°C; [α]_D +18 (c 0.8, CHCl₃), +7 (c 0.85, hexane); ¹H NMR (300 MHz, CDCl₃, TMS) δ (ppm) 7.81 (2H, m), 7.69 (2H, m), 4.19 (1H, q, *J* = 7.2 Hz), 1.52 (3H, d, *J* = 7.2 Hz), 0.99 (9H, s); ¹³C NMR (100 MHz, CDCl₃, TMS), δ (ppm): 169.503, 169.366, 134.110, 133.864, 132.500, 131.750, 123.369, 123.110, 56.368,

36.434, 27.734, 13.361; MS (EI): m/z 216 (5), 174 (100), 160 (9), 130 (21).

(S)-2-(sec-butyl)isoindoline-1,3-dione (2b) yield 86%; m.p.=42–44°C; $[\alpha]_D^{+17}$ (c 0.97, CHCl₃), +17 (c 1.39, CH₃OH), +16 (c 2.0, hexane); ¹HNMR (300 MHz, CDCl₃, TMS) δ (ppm) 7.81 (2H, m), 7.70 (2H, m), 4.26 (1H, ses, J=8.4 Hz), 2.05 (1H, m), 1.79 (1H, m), 1.47 (3H, d J=5.6 Hz), 0.88 (3H, m); ¹³CNMR (300 MHz, CDCl₃, TMS) δ (ppm) 168.8, 134.0, 132.2, 123.2, 49.3, 27.0, 18.6, 11.5; MS (EI): m/z 203 (12), 174 (100), 147 (10), 130 (24).

(S)-2-(3-methylbutan-2-yl)isoindoline-1,3-dione (2c) yield 25%; $[\alpha]_D^{+25}$ (c 1.12, CHCl₃), +21 (c 0.85, CH₃OH), +22 (c 0.92, hexane); ¹HNMR (300 MHz, CDCl₃, TMS) δ (ppm) 7.81 (2H, m), 7.69 (2H, m), 3.93 (1H, m), 2.37 (1H, m), 1.45 (3H, d, J=6.8 Hz), 1.01 (3H, d, J=6.4 Hz), 0.81 (3H, d, J=6.4 Hz); ¹³CNMR (300 MHz, CDCl₃, TMS) δ (ppm) 168.8, 134.0, 132.1, 123.3, 53.9, 31.3, 20.4, 20.3, 16.9; MS (EI): m/z 217 (4), 174 (100), 147 (9), 130 (24).

(S)-2-(1-cyclohexylethyl)isoindoline-1,3-dione (2d) yield 42%; $[\alpha]_D^{+10}$ (c 1.120 CHCl₃); ¹HNMR (400 MHz, CDCl₃, TMS) δ (ppm) 7.82 (2H, m), 7.70 (2H, m), 4.01 (1H, m), 2.05 (1H, m), 1.93 (1H, m), 1.77 (1H, m), 1.64 (2H, m), 1.52 (1H, m), 1.46 (3H, m), 1.30 (1H, m), 1.14 (2H, m), 0.943 (2H, m); ¹³CNMR (100 MHz, CDCl₃, TMS) δ (ppm) 168.9, 134.0, 132.1, 123.2, 52.6, 40.2, 30.8, 30.3, 26.3, 26.0, 25.9, 16.6; MS (EI): m/z: 174 (100), 130 (22).

Methyl (S)-2-(1,3-dioxoisindolin-2-yl)propanoate (2e) yield 53%; $[\alpha]_D^{-17}$ (c 1.0, CHCl₃), -22 (c 1.0, CH₃OH), -21 (c 1.0, hexane); ¹HNMR (500 MHz, CDCl₃, TMS) δ (ppm) 7.86 (2H, dd, J=3, 5 Hz), 7.74 (2H, dd, J=3, 5 Hz), 4.98 (1H, q, J=7.5 Hz), 3.73 (3H, s), 1.69 (3H, t, J=7.5 Hz); ¹³CNMR (500 MHz, CDCl₃, TMS) δ (ppm) 170.44, 167.62, 134.41, 132.16, 123.73, 53.00, 47.63, 15.51. MS (EI): m/z: 233 (3), 174 (100), 130 (20).

Methyl (S)-2-(1,3-dioxoisindolin-2-yl)-3,3-dimethylbutanoate (2f) yield 23%; m.p.=78–80°C; $[\alpha]_D^{-58}$ (c 0.9, CHCl₃); ¹HNMR (500 MHz, CDCl₃, TMS) δ (ppm) 7.88 (2H, dd, J=3, 5.5 Hz), 7.75 (2H, dd, J=3, 5.5 Hz), 4.64 (1H, s), 3.67 (3H, s), 1.18 (9H, s); ¹³CNMR (500 MHz, CDCl₃, TMS) δ (ppm) 168.52, 168.24, 134.42, 132.00, 123.81, 59.87, 52.28, 36.06, 29.94, 28.06; MS (EI): m/z 219 (65), 187 (100), 132 (34), 104 (19).

Methyl (S)-2-(1,3-dioxoisindolin-2-yl)-4-methylpentanoate (2g) yield 30%; m.p.=62–64°C; $[\alpha]_D^{+6}$ (c 0.8, CHCl₃); ¹HNMR (300 MHz, CDCl₃, TMS) δ (ppm) 7.86 (2H, m), 7.72 (2H, m), 4.86 (1H, dd, J=4, 11.2 Hz), 2.29 (1H, m), 1.90 (1H, m), 1.45 (1H, m), 1.41 (9H, s), 0.90 (6H, m); ¹³CNMR (100 MHz, CDCl₃, TMS) δ (ppm): 170.472, 167.938, 134.381, 132.028, 123.724, 52.918, 50.787, 37.455, 25.240, 23.368, 21.201; MS (EI): m/z 216 (91), 174 (35), 160 (100), 130 (14).

t-Butyl (S)-2-(1,3-dioxoisindolin-2-yl)-3-methylbutanoate (2h) yield 40%; m.p.=82–84°C; $[\alpha]_D^{-10}$ (c 0.94, CHCl₃); ¹HNMR (500 MHz, CDCl₃, TMS) δ (ppm) 7.87 (2H, dd, J=3, 5.5 Hz), 7.74 (2H,

dd, J=3, 5.5 Hz), 4.50 (1H, d, J=8.5 Hz), 2.73 (1H, m), 1.42 (9H, s), 1.14 (3H, d, J=6.5 Hz), 0.91 (3H, d, J=6.5 Hz); ¹³CNMR (500 MHz, CDCl₃, TMS) δ (ppm) 168.18, 168.05, 134.31, 132.05, 123.67, 82.42, 58.90, 28.79, 28.15, 21.31, 19.87; MS (EI): m/z 230 (2), 202 (100), 160 (18), 148 (24), 130 (20), 104 (10), 57 (30).

(R)-2-(sec-butyl)isoindoline-1,3-dione (2i) Yield 52%; $[\alpha]_D^{-16}$ (c 1.2 CHCl₃), ¹HNMR (400 MHz, CDCl₃, TMS) δ (ppm) 7.818 (2H, m), 7.701 (2H, m), 4.265 (1H, sx, J=7.2 Hz), 2.056 (1H, m), 1.795 (1H, m), 1.472 (3H, d, J=6.8 Hz), 0.883 (3H, t, J=7.2 Hz); ¹³CNMR (100 MHz, CDCl₃, TMS) δ (ppm) 168.81, 133.98, 132.23, 123.22, 49.30, 27.06, 18.61, 11.47; MS (EI): m/z 203 (M+), 174 (100), 147, 130, 76.

2-((1S,2S,5R)-2-isopropyl-5-methylcyclohexyl)isoindoline-1,3-dione (2j) yield 60%; $[\alpha]_D^{+4}$ (c 1.0 CHCl₃), ¹HNMR (400 MHz, CDCl₃, TMS) δ (ppm) 7.749 (2H, m), 7.635 (2H, m), 4.726 (1H, m), 2.151 (1H, m), 1.844 (2H, m), 1.688 (2H, m), 1.289 (2H, m), 0.796 (11H, m); ¹³CNMR (100 MHz, CDCl₃, TMS) δ (ppm): 188.897, 169.959, 134.058, 123.252, 49.795, 45.622, 41.611, 35.227, 30.058, 27.052, 26.298, 22.859, 21.794, 21.258; MS (EI): m/z 285 (M+), 200 (100), 160, 148, 130, 95.

Ethyl (R)-2-(1,3-dioxoisindolin-2-yl)propanoate (2k) yield 55%; $[\alpha]_D^{+5}$ (c 1.0 CHCl₃), ¹HNMR (400 MHz, CDCl₃, TMS) δ (ppm) 7.753 (2H, m), 4.971 (1H, q, J=7.2 Hz), 4.218 (2H, d, J=6.8 Hz), 1.702 (3H, d, J=7.2 Hz), 1.688 (2H, m), 1.238 (3H, t, J=6.8 Hz); ¹³CNMR (100 MHz, CDCl₃, TMS) δ (ppm): 169.899, 167.655, 134.373, 132.113, 123.683, 62.066, 47.781, 15.475, 14.297; MS (EI): m/z 247 (M+), 174 (100), 147, 130, 104, 76.

(R)-2-(but-3-yn-2-yl)isoindoline-1,3-dione (2l) yield 57%; $[\alpha]_D^{-5.6}$ (c 1.0 CHCl₃); ¹HNMR (400 MHz, CDCl₃, TMS) δ (ppm) 7.756 (2H, dd, J=3.2, 5.2 Hz), 7.664 (2H, dd, J=3.2; 5.2 Hz), 5.149 (1H, qrd, J=7.2, 7.4 Hz), 2.281 (1H, d, J=2.4 Hz), 1.648 (3H, d, J=7.2 Hz); ¹³CNMR (100 MHz, CDCl₃, TMS) δ (ppm): 167.114, 134.369, 132.048, 123.667, 81.289, 71.435, 37.088, 37.031, 20.277; MS (EI): m/z 199 (M+), 184 (100), 171, 130, 76.

Conflicts of interest

There are no conflicts to declare.

Acknowledgements

This research was supported by Project PON RI 2014-2020 BIOFEEDSTOCK (grant number ARS01_00985) financed by MIUR.

Notes and references

- 1 (a) N. Berova, L. Di Bari, G. Pescitelli, *Chem. Soc. Rev.*, 2007, **36**, 914–931. (b) N. Berova, P. L. Polavarapu, K. Nakanishi, R. W. Woody, Eds., *Comprehensive Chiroptical Spectroscopy*, John Wiley & Sons, Inc.: Hoboken, NJ, USA. 2012, Vols. 1 and 2.
- 2 N. Berova, G. A. Ellestad, N. Harada, in *Comprehensive Natural Products II Chemistry and Biology*, Mander, L., Lui, H.-W., Eds., Elsevier: Oxford, 2010; Vol. 9, Chapter 4, pp 91–146.
- 3 S. Superchi, C. Rosini, G. Mazzeo, E. Giorgio, in *Comprehensive Chiroptical Spectroscopy*, N. Berova, P. L. Polavarapu, K. Nakanishi, R. W. Woody, Eds. John Wiley & Sons, Inc.: Hoboken, NJ, USA. 2012, Vol. 2, Chapter 12, pp 421–427.
- 4 P.L. Polavarapu, *Chem. Rec.*, 2007, **7**(2), 125–136.
- 5 For general discussion of the *ab initio* calculation of chiroptical properties: (a) J. Autschbach, *Chirality*, 2009, **21**, E116–E152. (b) J. Autschbach, L. Nitsch-Velasquez, M. Rudolph, *Top. Curr. Chem.*, 2011, **298**, 1–98; (c) T. D. Crawford, *Theor. Chem. Acc.* 2006, **115**, 227–245.
- 6 P. L. Polavarapu, *Chirality*, 2002, **14**, 768–781.
- 7 P. Norman, K. Ruud, T. J. Helgaker, *Chem. Phys.*, 2004, **120**, 5027–5035.
- 8 (a) J. Autschbach, in *Comprehensive Chiroptical Spectroscopy*, N. Berova, P. L. Polavarapu, K. Nakanishi, R. W. Woody., John Wiley & Sons, Inc.: Hoboken, NJ, 2012, pp 593–642. (b) L. Goerigk, H. Kruse, S. Grimme, in *Comprehensive Chiroptical Spectroscopy*, N. Berova, P. L. Polavarapu, K. Nakanishi, R. W. Woody., John Wiley & Sons, Inc.: Hoboken, NJ, 2012, pp 643–673. (c) G. Pescitelli, T. Bruhn, *Chirality*, 2016, **28**, 466–474.
- 9 P. Stephens, F. Devlin, J. Pan, *Chirality*, 2007, **20**, 643–663.
- 10 For some recent reviews see: (a) G. Bringmann, T. Bruhn, K. Maksimenka, Y. Hemberger, *Eur. J. Org. Chem.*, 2009, 2717–2727. (b) X.C. Li, D. Ferreira, Y. Ding, *Curr. Org. Chem.*, 2010, **14**, 1678–1697. (c) G. Pescitelli, T. Kurtán, U. Flörke, K. Krohn, *Chirality*, 2009, **21**, E181–E201. (d) Y. He, B. Wang, R.K. Dukor, L.A. Nafie, *Appl. Spectr.*, 2011, **65**, 699–723. (e) Z. Sheng-Ding, S. Lan, L. Du-Qiang, Z. Hua-Jie, *Curr. Org. Chem.*, 2011, **15**, 1843–1862. (f) A.E. Nugroho, H. Morita, *J. Nat. Med.*, 2014, **68**, 1–10. (g) J.M. Batista Jr, E.W. Blanch, V.d.S. Bolzani, *Nat. Prod. Rep.*, 2015, **32**, 1280–1302. (h) S. Superchi, P. Scafato, M. Górecki, G. Pescitelli, *Curr. Med. Chem.*, 2018, **25**, 287–320.
- 11 For some examples from our group see: (a) A. Evidente, S. Superchi, A. Cimmino, G. Mazzeo, L. Mugnai, D. Rubiales, A. Andolfi, A. M. Villegas-Fernández, *Eur. J. Org. Chem.*, 2011, 5564–5570. (b) G. Mazzeo, E. Santoro, A. Andolfi, A. Cimmino, P. Troselj, A. G. Petrovic, S. Superchi, A. Evidente, N. Berova, *J. Nat. Prod.*, 2013, **76**, 588–599. (c) S. Santoro, S. Superchi, F. Messina, E. Santoro, O. Rosati, C. Santi, M. C. Marcotullio, *J. Nat. Prod.*, 2013, **76**, 1254–1259. (d) G. Mazzeo, A. Cimmino, A. Andolfi, A. Evidente, S. Superchi, *Chirality*, 2014, **26**, 502–508. (e) E. Santoro, F. Messina, M. C. Marcotullio, S. Superchi, *Tetrahedron*, 2014, **70**, 8033–8039. (f) E. Santoro, G. Mazzeo, A. G. Petrovic, A. Cimmino, J. Koshoubu, A. Evidente, N. Berova, S. Superchi, *Phytochemistry*, 2015, **116**, 359–366. (g) M. Evidente, E. Santoro, A. G. Petrovic, A. Cimmino, J. Koshoubu, A. Evidente, N. Berova, S. Superchi, *Phytochemistry*, 2016, **130**, 328–334. (h) M. Evidente, A. Cimmino, C. Zonno, M. Masi, E. Santoro, S. Vergura, A. Berestetskiy, S. Superchi, M. Vurro, A. Evidente, *Tetrahedron*, 2016, **72**, 8502–8507. (i) E. W. Coronado-Aceves, G. Gigliarelli, A. Garibay-Escobar, R. E. Robles Zepeda, M. Curini, J. López Cervantes, C. I. Espitia-Pinzón, S. Superchi, S. Vergura, M. C. Marcotullio, *J. Ethnopharmacol.*, 2017, **206**, 92–100.
- 12 (a) P. J. Stephens, J.-J. Pan, F. J. Devlin, M. Urbanová, J. Hájíček, *J. Org. Chem.*, 2007, **72**, 2508–2524. (b) P. L. Polavarapu, *Chirality*, 2007, **20**, 664–672. (c) P. Scafato, F. Caprioli, L. Pisani, D. Padula, F. Santoro, G. Mazzeo, S. Abbate, F. Lebon, G. Longhi, *Tetrahedron*, 2013, **69**, 10752–10762.
- 13 (a) S. Grimme, *Chem. Phys. Lett.*, 2001, **339**, 380–388. (b) P. J. Stephens, F. J. Devlin, J. R. Cheeseman, M. J. Frisch, *J. Phys. Chem. A*, 2001, **105**, 5356–5371; (c) M. Srebro, N. Govind, W. A. de Jong, J. Autschbach, *J. Phys. Chem. A*, 2011, **115**, 10930–10949.
- 14 (a) C. Wolf and K. W. Bentley, *Chem. Soc. Rev.*, 2013, **42**, 5408–5424 and reference therein; (b) D. Pasini and A. Nitti, *Chirality*, 2016, **28**, 116–123; (c) L. You, D. Zha, E. V. Anslyn, *Chem. Rev.* 2015, **115**, 7840–7892.
- 15 (a) S. Superchi, D. Casarini, A. Laurita, A. Bavoso, C. Rosini, *Angew. Chem. Int. Ed. Engl.*, 2001, **40**, 451. (b) P. Scafato, S. Superchi, *Chirality*, 2010, **22**, E3–E10. (c) E. Santoro, S. Vergura, P. Scafato, S. Belviso, M. Masi, A. Evidente, S. Superchi, *J. Nat. Prod.* 2020, accepted.
- 16 (a) S. Superchi, R. Bisaccia, D. Casarini, A. Laurita, C. Rosini, *J. Am. Chem. Soc.*, 2006, **128**, 6893. (b) S. Vergura, P. Scafato, S. Belviso, S. Superchi, *Chem. Eur. J.*, 2019, **25**, 5682–5690.
- 17 (a) S. Vergura, L. Pisani, P. Scafato, D. Casarini, S. Superchi, *Org. Biomol. Chem.*, 2018, **16**, 555–565. (b) L. Pisani, C. Bochicchio, S. Superchi, P. Scafato, *Eur. J. Org. Chem.* 2014, 5939–5945.
- 18 (a) S. Superchi, M. I. Donnoli, C. Rosini, *Org. Lett.*, 1999, **1**, 2093. (b) S. Superchi, D. Casarini, C. Summa, C. Rosini, *J. Org. Chem.*, 2004, **69**, 1685–1694.
- 19 S. Tartaglia, D. Padula, P. Scafato, L. Chiummiento, C. Rosini, *J. Org. Chem.*, 2008, **73**, 4865–4873.
- 20 G. Mazzeo, P. Scafato, S. Superchi, C. Rosini, *Tetrahedron: Asymmetry* 2009, **20**, 2435–2437.

- 21 For some examples of derivatization with chromophoric moieties see: (a) S. Kuwahara, M. Nakamura, A. Yamaguchi, M. Ikeda and Y. Habata, *Org. Lett.*, 2013, **15**, 5738–5741. (b) J. Zhang, H. Gholami, X. Ding, M. Chun, C. Vasileiou, T. Nehira and B. Borhan, *Org. Lett.*, 2017, **19**, 1362–1365. (c) J. M. Dragna, G. Pescitelli, L. Tran, V. M. Lynch, E. V. Anslyn and L. Di Bari, *J. Am. Chem. Soc.*, 2012, **134**, 4398–4407. (d) K. W. Bentley, Y. G. Nam, J. M. Murphy and C. Wolf, *J. Am. Chem. Soc.*, 2013, **135** (48), 18052–18055; (e) K. W. Bentley, L. A. Joyce, E. C. Sherer, H. Sheng, C. Wolf and C. J. Welch, *J. Org. Chem.*, 2016, **81**, 1185–1191.
- 22 P. Kocienski, *Protective Groups*, Thieme: Stuttgart, 1994, pp. 186–189.
- 23 N. Harada, K. Nakanishi, N. Berova, in *Comprehensive Chiroptical Spectroscopy*, N. Berova, R. W. Woody, P. Polavarapu, K. Nakanishi, Eds., Wiley: New York, 2012, Vol. 1, pp. 115–166.
- 24 J. Gawronski, F. Kazmierczak, K. Gawronska, U. Rychlewska, B. Nordén, A. Holmén, *J. Am. Chem. Soc.*, 1998, **120**, 12083–12091.
- 25 (a) J. Gawronski, F. Kazmierczak, K. Gawronska, P. Skowronek, J. Waluk, J. Marczyk, *Tetrahedron*, 1996, **52**, 13201–13214. (b) J. Gawronski, J. Grajewski, J. Drabowicz, M. Mikolajczyk, *J. Org. Chem.*, 2003, **68**, 9821–9822.
- 26 N. Harada, K. Nakanishi, *Circular Dichroic Spectroscopy - Exciton Coupling in Organic Stereochemistry*. University Science Books: Mill Valley, CA, 1983.
- 27 F. Kazmierczak, K. Gawronska, U. Rychlewska, J. Gawronski, *Tetrahedron: Asymmetry*, 1994, **5**, 527–530.
- 28 Z. Li, Z. Zhou, L. Wang, Q. Zhou, C. Tang, *Tetrahedron: Asymmetry*, 2002, **13**, 145–148.
- 29 (a) J. Tomasi, B. Mennucci, R. Cammi, *Chem. Rev.*, 2005, **105**, 2999–3093. (b) B. Mennucci, R. Cammi, Continuum Solvation Models in Chemical Physics: From Theory to Applications, Wiley, Chichester, 2007.
- 30 J. Cerezo, F. J. Avila Ferrer, G. Prampolini, F. Santoro, *J. Chem. Theory Comput.*, 2015, **11**, 5810–5825.
- 31 (a) G. Pescitelli, V. Barone, L. Di Bari, A. Rizzo, F. Santoro, *J. Org. Chem.*, 2013, **78**, 7398–7405. (b) D. Padula, G. Pescitelli, *Molecules*, 2018, **23**, 128.
- 32 Spartan '02, Wavefunction, Inc.: Irvine, CA, 2002.
- 33 S. Belviso, E. Santoro, F. Lejl, D. Casarini, C. Villani, R. Franzini, S. Superchi, *Eur. J. Org. Chem.*, 2018, 4029–4037.
- 34 M. J. J. Frisch, G. W. Trucks, H. B. Schlegel, G. E. Scuseria, M. A. Robb, J. R. Cheeseman, G. Scalmani, V. Barone, B. Mennucci, G. A. Petersson, H. Nakatsuji, M. Caricato, X. Li, H. P. Hratchian, A. F. Izmaylov, J. Bloino, G. Zheng, J. L. Sonnenberg, M. Hada, M. Ehara, K. Toyota, R. Fukuda, J. Hasegawa, M. Ishida, T. Nakajima, Y. Honda, O. Kitao, H. Nakai, T. Vreven, J. A. Montgomery, J. E. Peralta, F. Ogliaro, M. Bearpark, J. J. Heyd, E. Brothers, K. N. Kudin, V. N. Staroverov, R. Kobayashi, J. Normand, K. Raghavachari, A. Rendell, J. C. Burant, S. S. Iyengar, J. Tomasi, M. Cossi, N. Rega, M. M. Millam, M. Klene, Knox, J. E. Cross, J. B. Bakken, V. Adamo, C. Jaramillo, J. Gomperts, R. Stratmann, R. E. Yazyev, O. Austin, A. J. Cammi, R. Pomelli, C. Ochterski, J. W. Martin, R. L. Morokuma, K. Zakrzewski, V. G. Voth, G. A. Salvador, P. Dannenberg, J. J. Dapprich, S. Daniels, A. D. Farkas, J. B. Foresman, J. B. Ortiz, J. V. Cioslowski, J. Fox, D. J. Gaussian 09, Revision D.01. Gaussian, Inc., Wallingford CT.
- 35 T. Bruhn, A. N. U. Schaumlöffel, Y. Hemberger, G. Bringmann, *Chirality*, 2013, **25**, 243–249.

Transformation of chiral UV-transparent amines and alcohols to phthalimides enhances their chiroptical response allowing absolute configuration assignment by ECD computation

View Article Online
DOI: 10.1039/D0OB00052C

